

## NUMERICAL SIMULATION AND AUXILIARY ENTRAINMENT OF STEAM EJECTORS

Yongzhi Tang, Zhongliang Liu<sup>§</sup>, Yanxia Li, Weina Fu, Hongqiang Wu  
College of Environmental & Energy Engineering  
Beijing University of Technology, Beijing 100124, China

<sup>§</sup>Correspondence author. Fax: +86 10 67392774 Email: liuzhl@bjut.edu.cn

**ABSTRACT** The numerical results disclose that there are several locally low-pressure areas inside a well-designed steam ejector. Based on this finding, a so-called auxiliary entrainment technology is proposed to entrain extra entrained steam by connecting these locally low-pressure areas to the suction chamber of the entrained steam. Then numerical simulations are carried out of different auxiliary entrainment schemes. The results reveal that although the auxiliary entraining entrance of the mixing chamber auxiliary entrainment can entrain some low-pressure steam into the ejector, the auxiliary entrainment results in a decrease in the entrained steam mass flow rate of the main entrained steam entrance that is greater than the auxiliary entrainment steam mass flow rate. However, it is also disclosed that the throat auxiliary entrainment does increase the entrainment ratio of the steam ejector. The best result obtained in our simulation is that the ejector entrainment ratio is increased by 3.68%. Therefore, it may be concluded that auxiliary entrainment may be an effective way for improving the performance of steam ejectors, although its feasibility needs proving experimentally.

## INTRODUCTION

Steam ejector is a kind of fluid machinery which entrains low-pressure steam (entrained steam) by consuming a certain amount of high-pressure primary steam. In some situations, the application of ejectors helps to recovery a large part of the waste heat of the entrained steam and thus produce energy saving. Therefore steam ejectors have been finding more and more applications in various industrial processes including seawater desalination, power, and chemical engineering. Many scholars have comprehensively analyzed the influences of working and structural parameters on the steam ejector performance, the internal flow field and shock wave phenomena using the numerical simulation and experimental methods [*e.g.*, Xia *et al.* 2014]. Many efforts have also been made to improve the steam ejector performance by changing its structure [*e.g.* Wu *et al.* 2014 and Fu *et al.* 2016].

The present structure of steam ejectors basically consists of an inlet for primary working steam, an inlet for entrained steam and an outlet for mixed steam. The structure takes the full use of the pressure difference between the mixing chamber and the entrained steam that is formed from high speed flow of the working steam. However, our numerical simulation disclosed that there still exist some low-pressure regions inside the ejector that might be used to suck a certain amount of the entrained steam and thus to increase the entrainment ratio which is a main indicator of steam

ejector performance. Therefore, in this paper, a new method that takes the full use of the possible low-pressure region inside ejectors to entrain the additional low-pressure steam by adding auxiliary entrainment openings in the ejector is proposed and its effectiveness is verified by our detailed numerical simulation of internal flow field under various conditions.

## STRUCTURE AND CFD MODEL OF STEAM EJECTOR

**Structure of the Ejector** The auxiliary entrainment type steam ejector is mainly composed of the following five parts: the primary nozzle, the suction chamber, the mixing chamber, the ejector throat, the diffuser and the auxiliary entraining entrance. For simplifying CFD model, the lateral entrance of the entrained fluid is replaced by an axial annular entrance, and the auxiliary entrained fluid is introduced into the ejector by radial circular entrances. If the auxiliary entraining entrance is closed, then its influences on the steam ejector are neglected and the ejector is taken as a conventional one. The external wall of the steam ejector is assumed to be adiabatic. In this way, the steam ejector is simplified to be two-dimensional axisymmetric, as shown in Figure 1. The auxiliary entraining entrance whose width is 4 mm is manufactured in the mixing chamber, the ejector throat. The detailed geometric parameters of the steam ejector are omitted here. The designed operation conditions are: the primary steam pressure  $p_w=500$  kPa, the entrained steam pressure  $p_e=20$  kPa and the outlet mixing steam pressure  $p_c=40$  kPa, the entrainment ratio  $\omega=0.6785$ .

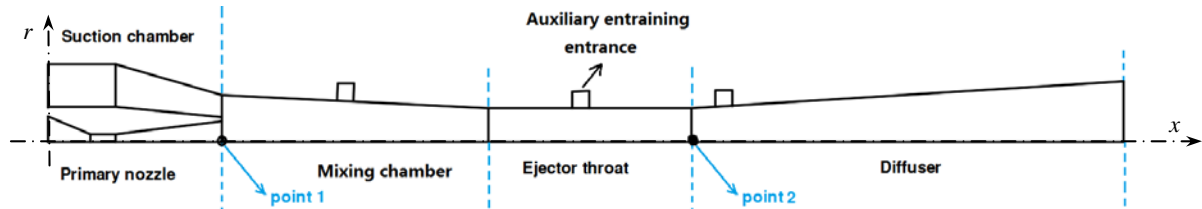


Figure 1 Steam ejector with auxiliary entraining entrances

**CFD Model** Due to the complexity of the structure of the steam ejector, it is almost impossible to discretize it as a whole. Therefore, the ejector is divided into several sections according to their geometry characteristics, and then is performed over each section using grid adaptive technique. Grid refining is adopted where the pressure, velocity, temperature and other flow parameters might be of large gradient. The ejector is divided into 109511 meshes after grid independent validation which will be introduced later on. The commercial software FLUENT is used with the help of high performance server. The implicit and unsteady solver with realizable  $k-\varepsilon$  turbulence model is used [Bartosiewicz *et al.* 2005 and Yang *et al.* 2012]. The outlet and the inlet of the steam ejector are taken as pressure boundary condition. The fluid (water vapor) is regarded as ideal gas, and the wall is treated as no-slip and adiabatic. The SIMPLE algorithm is used to solve the physical and mathematical model. In order to ensure convergence, the value of important relaxation factors is carefully chosen and tried. The iteration convergence criterion is the residual of related parameters with the full consideration that the inlet and outlet mass flow rate remain unchanged as the iteration proceeds. The residual for pressure and velocity is less than  $10^{-5}$  and the change in the mass flow rate of the inlet and outlet should be less than  $10^{-8}$  kg/s each iteration.

To ensure the accuracy and reliability of the numerical results, the grid independence test is made. Numerical simulation was made of the ejector without auxiliary entraining opening with 4 different grids. The results showed that with a grid number of 109511 the simulation reliability and accuracy could be guaranteed.

**Numerical Simulation of Designed Ejector** A systematic numerical simulation was carried out of the designed ejector under the designed operation conditions ( $p_w=500$  kPa,  $p_e=20$  kPa and  $p_c=40$  kPa). Fig. 2 presents the pressure contour inside the steam ejector. It can be seen from the figure that inside the ejector, beside the low pressure area that is effective for sucking the entrained steam in the immediate downstream of the main nozzle, at least three areas where the pressure is as low as that of the

immediate downstream of the main nozzle. Among these three low-pressure areas, the one in the mixing chamber (denoted by letter A) and the one in the ejector throat (denoted by letter B) are of the largest. The detailed analysis of our numerical simulation results shows that the pressure difference between these local low-pressure areas and the entrained steam can be as large as 13 kPa approximately. This remind us we can connect these low-pressure areas with the entrained steam with external pipes or passages and utilize the pressure difference between these local low-pressure areas and the entrainment steam to suck more entrained steam into the ejector. In this way, the mass flow rate of the entrained steam is increased and the working performance of the steam ejector is improved. This is the theoretical basis and starting point for our auxiliary entrainment technical solution.

## AUXILIARY ENTRAINMENT

In the last section, the analysis of our numerical simulation results shows that there are still several local low-pressure areas located in different axial positions of the steam ejector under the design conditions. To use the pressure difference between these additional low-pressure areas and the entrained steam, it is proposed an auxiliary entrainment opening is manufactured and connected to the entrained steam in those locations of the ejector that a usable low-pressure area, that is, the pressure of this position is lower than that of the entrained steam, may appear. It is expected that through these auxiliary entrainment opening more entrained steam can be drawn into the ejector helping to improve the ejector performance. For realizing auxiliary entrainment, one circular opening of 4mm-in-width that is used as the auxiliary entraining entrance is set at the mixing chamber ( $x$  from 65 mm to 69 mm), one at the ejector throat ( $x$  from 115 mm to 119 mm). Then numerical simulations were made to verify the feasibility of different auxiliary entrainment schemes.

To assess the effectiveness of auxiliary entrainment, two parameters are defined. One is mass flow rate increment  $\Delta m = m - m_0$ , where  $m$  and  $m_0$  are the mass flow rate of each inlet/outlet of the ejector with and without the auxiliary entrainment. For auxiliary entraining entrance,  $m_0 = 0$ , *i.e.*,  $\Delta m = m$ . Another is the entrainment ratio improvement  $\varepsilon$  which is defined as,

$$\varepsilon = \frac{\Delta \omega}{\omega_0} \times 100\% = \frac{\omega - \omega_0}{\omega_0} \times 100\% \quad (1)$$

where  $\omega$  and  $\omega_0$  are the entrainment ratio with and without auxiliary entrainment.

**Mixing Chamber Auxiliary Entrainment** When the auxiliary entrainment opening is connected to the main entrainment steam cavity, the numerical results show that a certain quantity of the entrained steam is sucked into the ejector through this opening (2.389 g/s). However, the addition of this auxiliary entrainment opening results in a decrease in the main entrainment flow rate ( $\Delta m = -2.612$  g/s), and therefore, the net effect of the mixing chamber auxiliary entrainment is negative, it leads to the deterioration of the performance of the ejector. Actually, the entrainment ratio improvement is -4.21%.

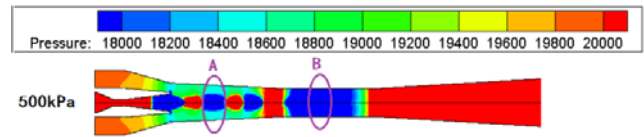


Figure 2 Pressure color map of the designed ejector working under the designed conditions

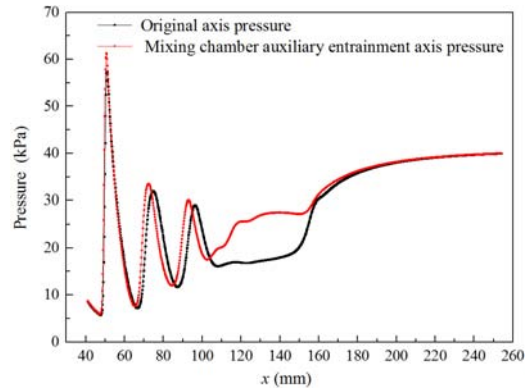


Figure 3 Pressure distribution with and without mixing chamber auxiliary entrainment

In order to find out the reason for this, Figure 3 presents the pressure distribution along the axial line of the ejector before and after adding the auxiliary entrainment in the mixing chamber. As one can see from the figure, adding the auxiliary entraining entrance has produced very important influences on the axial pressure distribution of the ejector. One of the influences is the average pressure of the mixing chamber ( $x = 41$  mm to  $x = 103.9$  mm) increases significantly, and this is the very reason why the steam mass flow of the main entrainment entrance is greatly reduced.

**Ejector Throat Auxiliary Entrainment** Ejector throat auxiliary entrainment is to open an auxiliary entraining entrance (denoted by letter B in Figure 1) in the low-pressure area of the ejector throat and make it directly connected to the entrained steam cavity, in the hope that extra entrained steam might be entrained into the ejector. The numerical simulation shows that a certain quantity of the entrained steam is sucked into the ejector through the auxiliary entrainment entrance (about 0.203 g/s). Although the simulation also shows that adding the auxiliary entrainment opening results in a decrease in the main entrainment flow rate ( $\Delta m = -0.009$  g/s), it is significantly smaller than the entrained steam flow rate of the auxiliary entrainment opening. Therefore, the net effect of the ejector auxiliary entrainment is to increasing the total entrained steam flow rate and to improve the performance of the ejector. The entrainment ratio improvement is 3.68%. Hence, adding the auxiliary entraining entrance in the ejector throat is a good practice for improving steam ejector performance.

Figure 4 compares the pressure distribution along the axial line of the ejector with and without adding the auxiliary entrainment at the ejector throat. As one can see, adding the auxiliary entrainment has little influence on the pressure distribution of the mixing chamber (from  $x=41$ mm to  $x=103.9$  mm) and the diffuser ( $x>151.9$ mm). This explains why adding the auxiliary entraining entrance has little effect on the entrained steam flow mass rate of the main entrainment entrance. However, the pressure in the throat section rises significantly after the auxiliary entraining entrance is added. This is because that a certain amount of the entrained steam is sucked into this area and this additional steam will certainly increase the local pressure.

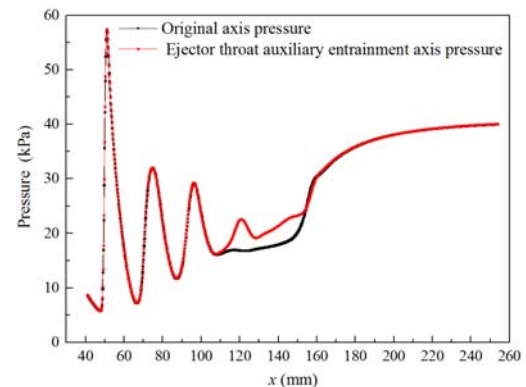


Figure 4 Pressure distribution with and without ejector throat auxiliary entrainment

## CONCLUSION

Although there exists a local low-pressure area in the mixing chamber and a certain amount of the entrained steam could be sucked into the ejector, the mixing chamber auxiliary entrainment has an adverse affect on the overall performance of the ejector. The throat auxiliary entrainment can entrain a certain amount of the entrained steam and it basically produces no negative effect on the mass flow rate of the entrained steam from the main entrainment entrance, the entrainment ratio improvement is as high as 3.68%. Therefore, adding the auxiliary entraining entrance in the throat section can effectively improve the steam ejector performance.

## ACKNOWLEDGEMENTS

This work is supported by Beijing Municipal Natural Science Foundation Project (No. 3162007) and the Beijing Municipal Science & Technology Plan Project (No. Z111100058911006).

## REFERENCE

- Bartosiewicz Y., Aidoun Z., Desevaux P. [2005], *Int. J of Heat and Fluid Flow*, Vol.26, pp 56-70.  
 Fu W.N., Li Y.X., Liu Z.L., Wu H.Q., Wu T.R. [2016], *Applied Thermal Engineering*, Volume 106, pp 1148–1156.  
 Wu H.Q., Liu Z.L., Han B. [2014], *Desalination*, Vol. 353, pp 15-20.  
 Xia Z.C., Li J.X., Gao D., Chen G.M. [2014], *J. of Refrigeration*, Vol. 35, pp 45-49.  
 Yang X., Long X., Yao X. [2012], *Int. J. of Thermal Sciences*, Vol. 56, pp 95-106.